DEVELOPMENTAL DYNAMICS 239:1995–2004, 2010

RESEARCH ARTICLE

Arterial and Venous Vessels Are Required for Modulating Developmental Relocalization and Laterality of the Interrenal Tissue in Zebrafish

Chih-Wei Chou,[1] Hsiao-Chu Hsu,[1] Sue-Ing Quek,[2] Woon-Khiong Chan,[2] and Yi-Wen Liu[1]*

During zebrafish embryogenesis, the endothelium signals to emergent bilateral interrenal primordia to converge toward the midline, yet the merged interrenal tissue has been found to be situated lateral to the midline. We show in this study that bilateral interrenal tissue clusters fused at the central midline, before relocating laterally to be juxtaposed between the dorsal aorta and the posterior cardinal vein. In *ets1b* morphants where the midtrunk vasculature failed to assemble, various degrees of interrenal fusion defects were displayed, and the interrenal laterality was lost. As either arterial or venous endothelium was specifically reduced, the interrenal tissue was defective in its relocalization and laterality, yet remained closely associated with the malformed vasculature. Our results showed evidence to support that assembly of the axial artery and vein, and its resulting vascular topology at the midtrunk, is required for patterning relocalization and laterality of the interrenal tissue after the initial medial fusion. *Developmental Dynamics 239:1995–2004, 2010.* © 2010 Wiley-Liss, Inc.

Key words: zebrafish; adrenal; interrenal; steroidogenic; endothelium; artery; vein; laterality; *ets1b*; *gridlock/hey2*

Accepted 4 May 2010

INTRODUCTION

Interactions between endothelial cells (EC) and the microenvironment are known to regulate organogenesis and pattern formation in the embryo (for a review see Cleaver and Melton, 2003; Nikolova et al., 2007; Red-Horse et al., 2007). The zebrafish, due to its optical clarity, has been shown to be a good model for observing the interplay between organs and vasculature during early development. Also, a vast array of mutants and morphants manifesting various types of vascular disorders has allowed a detailed genetic dissection of endothelial signals that modulate organogenesis. For example, in the developing zebrafish embryo, endothelium has been found to regulate cardiomyocyte movement during heart tube assembly (Holtzman et al., 2007), to provide guidance cues for defining the position of the thyroid gland (Alt et al., 2006), and to regulate the apicobasal polarization of hepatocytes (Sakaguchi et al., 2008). Furthermore, endothelium-derived signals play morphogenetic roles for the embryonic renal and interrenal organs (Serluca et al., 2002; Liu and Guo, 2006), while these two organs develop in a highly parallel manner.

The interrenal tissue, the teleostean counterpart of mammalian adrenal cortex, is derived from the embryonic kidney, or pronephros (Hsu et al., 2003; Chai et al., 2003). Although tissue organization and morphology of the interrenal tissue in zebrafish demonstrates species-specific differences from its mammalian counterpart, key mechanisms that control the interrenal organogenesis and steroidogenesis highly resemble those in mammals (for a review see Liu, 2007). In the zebrafish embryo, both kidney and interrenal tissue arise as bilateral clusters across the midline, and migrate centrally in a coordinated

Additional Supporting Information may be found in the online version of this article.

[1]Department of Life Science, Tunghai University, Taichung, Taiwan, R.O.C
[2]Department of Biological Sciences, National University of Singapore, Singapore

Grant sponsor: National Science Council (R.O.C.); Grant sponsor: NSC; Grant number: 96-2628-B-029-002-MY3; Grant sponsor: A*STAR-BMRC (Singapore); Grant number: BMRC07/1/21/19/527.

***Correspondence to: Yi-Wen Liu, Department of Life Science, Tunghai University, No. 181, Sec. 3, Taichung-Port Road, Taichung, 40704, Taiwan R.O.C. E-mail: dlslys@thu.edu.tw**

DOI 10.1002/dvdy.22335
Published online 28 May 2010 in Wiley InterScience (www.interscience.wiley.com).

fashion (Hsu et al., 2003). While central assembly of the pronephros requires the hemodynamic force (Serluca et al., 2002), medial migration of primordial interrenal cells toward the midline is regulated by the interrenal-associated endothelium, possibly prior to vessel formation (Liu and Guo, 2006). The converged interrenal tissue is located to the right of the midline, and juxtaposed between the dorsal aorta (DA) and the right branch of the posterior cardinal vein (PCV) (Liu and Guo, 2006). However, it remains unclear whether the initial merging point of bilateral interrenal clusters is at or to the right of the midline. Also, it could not be ruled out that the left interrenal cell cluster might disappear before reaching the midline, leaving the right cluster for subsequent morphogenesis. We hypothesized that in parallel with assembly of the DA and the PCV at the midtrunk area, the centrally-migrating primordial interrenal cells first fuse at the central midline, before a lateral relocalization to the right of the midline, resulting in a single interrenal tissue cluster "sandwiched" between the DA and the PCV. Also, developmental relocalization of the interrenal tissue after the convergence event could be modulated by its adjacent vessels. The functional differentiation of interrenal cells, detected by 3βHsd activity staining as early as 28 hpf, takes place approximately concurrent with the morphogenetic phase of interrenal relocalization, which implied that the endocrine function of steroid secretion might be ready right after the onset of blood circulation.

In order to validate the putative morphogenetic steps in our proposed model, we performed in situ hybridization (ISH) and transgenic reporter analyses to capture the morphology of bilateral interrenal tissues that were undergoing midline fusion. We also examined the interrenal phenotype in *ets1b* morphants where the trunk vasculature was severely disrupted, as well as in embryos with specific reduction in either arterial or venous cells. The results of our phenotypic analyses suggest that midline fusion and lateral relocalization take place in the process of embryonic interrenal morphogenesis, and these movements are dynamically regulated by the peri-interrenal endothelium, which participates in assembly of the DA and the PCV.

RESULTS AND DISCUSSION

The Midline Fusion of Primordial Interrenal Cells as Detected by Both ISH and Transgenic Reporter Analyses

The fusion and relocalizing processes of bilateral interrenal primordia were delineated through analyzing the expression of *ff1b* mRNA as well as the green fluorescence driven by *ff1b* promoter, immediately after the interrenal specification. *ff1b* (NR5A4) has been discovered to be the earliest gene expressed at the developing interrenal tissue (Chai et al., 2003; Hsu et al., 2003). *ff1b* is the orthologue of mammalian steroidogenic factor 1 (SF-1/Ad4BP; NR5A1), and the disruption of its expression leads to a complete ablation of the embryonic interrenal tissue. Earlier ISH results of detecting *ff1b* mRNA transcripts by using Fast Red chromogenic staining imply that bilateral interrenal cell clusters emerge at about 21-somite stage, and the convergence toward the midline is completed by 23-somite stage (Hsu et al., 2003; Liu et al., 2003). Those results, however, did not explicitly demonstrate the primary mechanism of interrenal asymmetry, and it could not be ruled out that the interrenal laterality could be due to asymmetric degeneration, apoptosis, or disassociation of one primordia. In order to address this issue, firstly we utilized NBT/BCIP staining to obtain better resolution of ISH in detecting the *ff1b* mRNA expression in embryos at the 21- to 26-somite stages. Consistent with the former studies, bilateral interrenal tissues were detectable in embryos as early as the 21-somite stage (Figs. 1A, 21S). In contrast, a single interrenal cell cluster of the shape as shown in Figure 1A, 22S, apparently formed by the fusion of bilateral clusters migrating toward the midline, was detected in embryos at the 22-somite stage. Subsequently, at approximately the 24-somite stage, some interrenal cells started to be displaced away from the midline (Fig. 1A, 24S), culminating in a single leaf-shaped interrenal tissue cluster localized to the right of the midline as viewed dorsally (ventral view shown in Fig. 1A, 26S).

To further validate the process of interrenal fusion and repositioning in the developing embryo, we performed a time-lapse confocal analysis on the embryo where the interrenal cells were traced by utilizing a *ff1b* promoter-driven green fluorescent line, *Tg(ff1bEx2:GFP)*. The interrenal identity of GFP-expressing cells in the *Tg(ff1bEx2:GFP)* embryo was verified by colocalization of the GFP expression with the 3βHsd enzymatic activity staining (Fig. 1B). At 32 hpf, most of the GFP-expressing cells near the third somite appeared as a leaf-shape cluster to the right of the midline as viewed dorsally, and the 3βHsd activity was detected in part of the GFP-expressing cells. This was consistent with our former results that 3βHsd activity is detected in some but not all of the *ff1b* -expressing interrenal cells during development (Chai et al., 2003; Liu et al., 2003). In some samples, a tiny cluster of GFP-expressing cells appeared to be dispersed from the main interrenal tissue and was localized at the left of the midline. This might be due to the differential rate of cell migration within the interrenal cell population. The *ff1b* promoter-driven fluorescence could be detected as early as the 21-somite stage, and a time-lapse confocal analysis was performed on the *Tg(ff1bEx2:GFP)* embryo starting from this stage (Fig. 1C). Bilateral rows of GFP-positive cells were also detected throughout the scanning period, which represented ectopic GFP expression at muscle pioneer cells, possibly due to the presence of an enhancer element near the site of transgene integration (Quek, 2009), and this domain of fluorescence weakened later at about 32 hpf. The live *Tg(ff1bEx2:GFP)* embryo was incubated at 23°C in order to slow down the developmental process for the purpose of clear observation. The bilateral interrenal clusters, as detected by *ff1b* promoter-driven GFP expression, started to fuse medially by 42 min after the onset of scanning. The interrenal morphology at the time of fusing was consistent with the

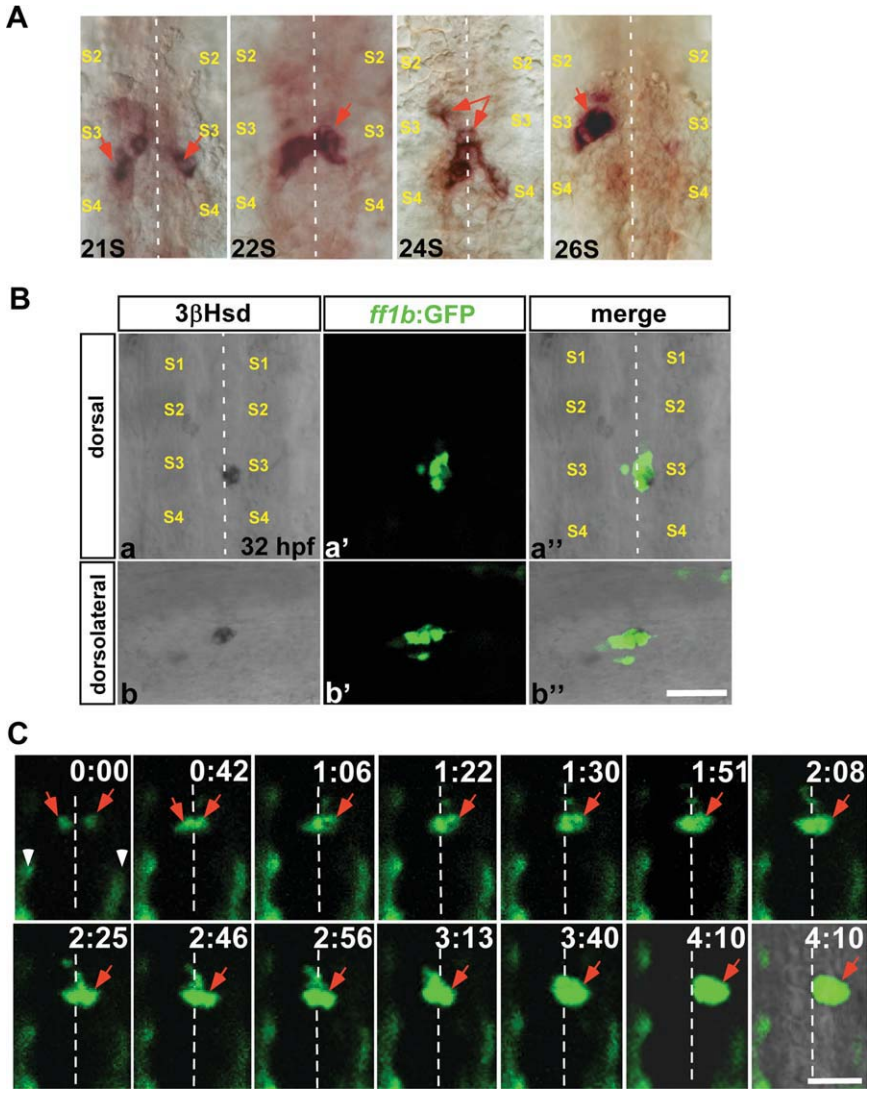

Fig. 1. The *ff1b*-expressing interrenal primordia during midline fusion and lateral repositioning. **A**: Ventral flat mount views of 21-somite (21S), 22-somite (22S), 24-somite (24S), and 26-somite (26S) stage embryos, which were subject to ISH for detecting *ff1b* mRNA, with anterior oriented to the top. **B**: The colocalization of steroidogenic activity and *ff1b*:GFP transgene expression at the interrenal tissue, in the *Tg(ff1bEx2:GFP)* embryo. Confocal images display the steroidogenic cells as detected by 3βHsd activity staining (a,b), and the green fluorescence driven by *ff1b* promoter (a′,b′), in a *Tg(ff1bEx2:GFP)* embryo at 32 hpf. The merged images of 3 μ-Hsd activity staining and GFP are shown in a″,b′. **a–a**″: Dorsal views with anterior to the top; (**b–b**″) dorsolateral views with anterior to the right. **C**: Confocal time-lapse imaging of the interrenal tissue in a live *Tg(ff1bEx2:GFP)* embryo. A dechorionated embryo at around 21-somite stages was mounted with the dorsal side up in 3% methyl cellulose. The fluorescent images were collected at 1-min intervals, and representative frames are shown. The last frame of the time series is a merge of fluorescent and bright-field images. Time is indicated by hours:minutes. Since the sample was kept at 23°C during observation, developmental stages cannot be accurately addressed. Each fluorescent image in B and C represents a projection of a consecutive z-stack encompassing the depth of the interrenal tissue. Both ISH and time-lapse *ff1b*:GFP analyses show that the interrenal primordia fuse at the midline prior to the lateral relocalization. Red arrows indicate *ff1b*-expressing interrenal primordia in A, and the *ff1b* promoter-driven interrenal-specific fluorescence in C. S2, S3, and S4, the second, third, and fourth somite, respectively. White arrowheads in C indicate ectopic GFP expression in muscle pioneer cells. White dotted lines indicate the position of the midline. Scale bar = 50 μM.

ff1b mRNA expression pattern as detected by ISH at the 22-somite stage in Figure 1A. By 1 hr, a fused interrenal tissue was found to be relocalized toward the right of the midline, with a tiny rostral cluster appearing to be dispersed from the main cluster. At this time, the fused interrenal tissue showed a 2.2-fold increase in size as compared to that which is summed from the bilateral clusters at time point 0:00 (Fig. 1C; see Supp. Fig. S1, which is available online), implying that *ff1b*-expressing cells from each of the bilateral interrenal tissue combined to result in a single interrenal tissue during the process of medial fusion. By 250 min after scanning, when the fused interrenal tissue was fully relocated to the right of the midline, the interrenal size expanded to about 2.8-fold of that right after the interrenal fusion, indicating active interrenal cell proliferation following the medial fusion event.

Altogether, both ISH and time-lapse transgenic reporter results support our hypothesis that medially migrating bilateral interrenal primordia first fuse at the central midline, and the merged interrenal tissue is subsequently relocalized to the right of the midline. It is then of interest to check how these morphogenetic movements could be modulated by the peri-interrenal vasculature.

Disrupted Formation of Trunk Vasculature Led to Defective Midline Fusion and Relocalization of the Interrenal Tissue

Subsequent to the medial migration and midline fusion, the interrenal tissue was laterally relocalized and juxtaposed between the DA and the right branch of the PCV (Fig. 2A–A″). Previously, it has been shown that central convergence as well as laterality of the interrenal tissue was normal in embryos injected with the antisense morpholino oligo against *cardiac troponin T2* (*tnnt2*) gene (Liu and Guo, 2006), where the blood flow is absent (Sehnert et al., 2002), suggesting that hemodynamic force might not be essential for the early interrenal morphogenetic movement. Instead, we propose here that right-sided laterality of the interrenal tissue might be correlated with patterning of the DA and the PCV at the mid-trunk. To test this hypothesis, we checked the embryonic interrenal morphology in *ets1b*-deficient embryos where the formation of trunk vasculature was

disrupted. Ets1-related protein (Etsrp; or Ets1b) has been identified to regulate endothelial but not hematopoietic development (Sumanas and Lin, 2006). Ets1b appears to function straight downstream of *clo* (Sumanas and Lin, 2006). Consistent with the former study, a mixed injection of two morpholino oligos against *ets1b* at a high dosage (15 ng) resulted in a complete loss of circulation, and severe elimination of endothelium (Fig. 2B′–D′) as verified by *fli1* promoter-driven vascular-specific GFP fluorescence in *Tg(fli1:EGFP)*^{Y1} embryos (Lawson and Weinstein, 2002). The remaining *fli1*-expressing cells in *ets1b* morphants were speculated to be aggregated angioblasts as a consequence of disrupted vasculogenesis, and appeared to display high affinity to the interrenal tissue (Fig. 2B′–D′,B″–D″). While the trunk vasculature was compromised, *ets1b* morphants displayed variable expressivity of interrenal convergence phenotype, which was accompanied by a loss of laterality (Fig. 2B–D). In contrast with the uniform interrenal convergence phenotype seen in angioblast-deficient *clo* mutant, that bilateral interrenal primordia fail to fuse and were separately located at two sides of the midline (Liu and Guo, 2006), we saw intermediate phenotypes shown as

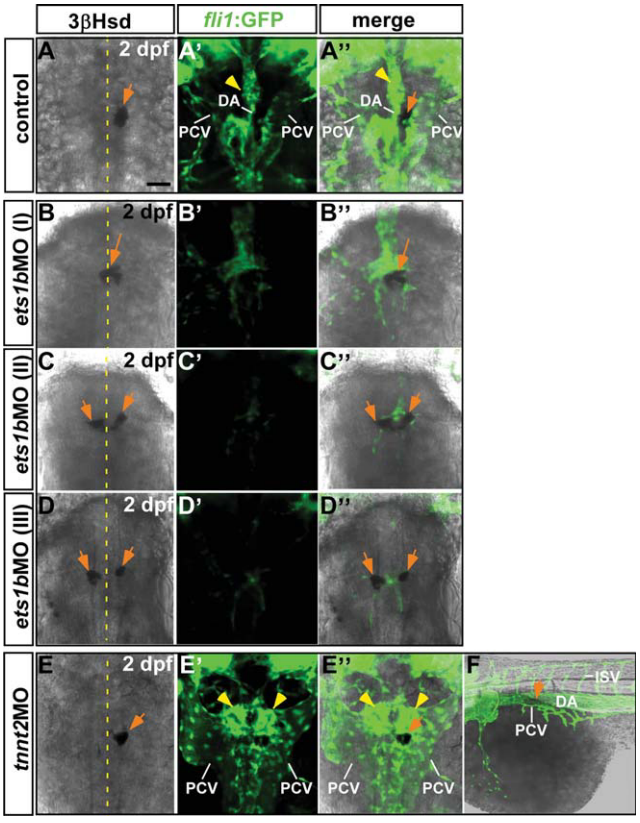

Fig. 2.

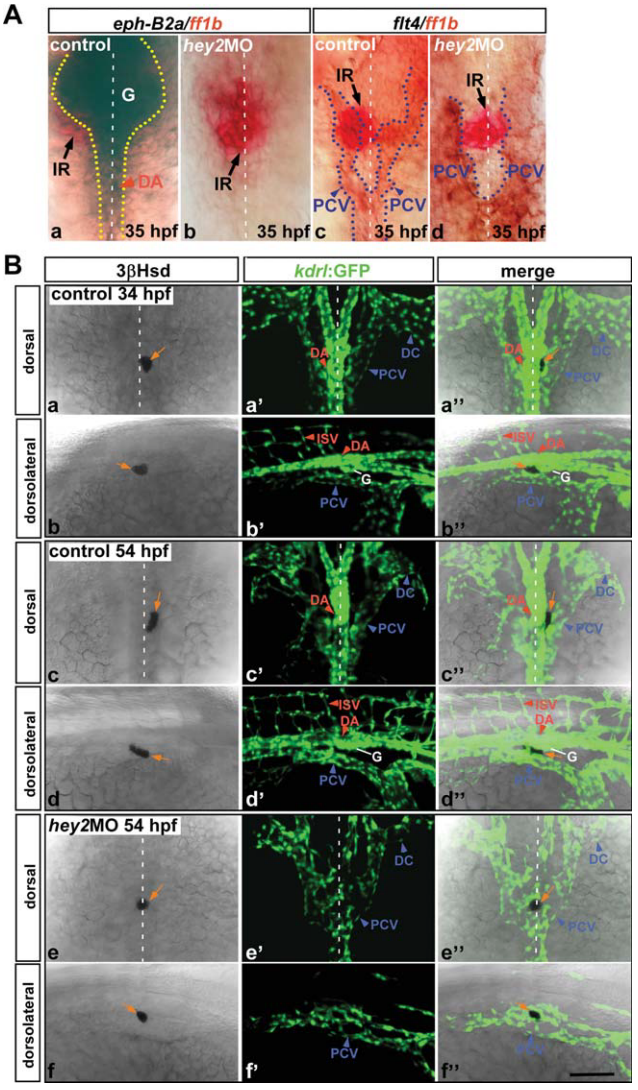

Fig. 3.

TABLE 1. Analysis of *ets1b* Morphant Phenotypes in 2-dpf *Tg(fli1:EGFP)*^{Y1} Embryos as Viewed From the Dorsal Side

		*ets1b*MO		Control	
Phenotype	Morphology of the interrenal tissue	No.	(%)	No.	(%)
Normal	Single cluster to the right of the midline	12	(11.3)	112	(96.6)
Class (I)	Single cluster from the midline fusion of bilateral ones	36	(34.0)	0	
Class (II)	Bilateral elongated clusters with caudal ends fusing at the midline	31	(29.2)	0	
Class (III)	Bilateral clusters across the midline	27	(25.5)	4	(3.4)
	Total	106		116	

reverse U-shape (class I in Fig. 2B) or V-shape (class II in Fig. 2C) interrenal clusters across the midline, which appeared to result from incomplete fusion. The most severe phenotype in class III (Fig. 2D) of *ets1b* morphants well resembled the interrenal morphology in the *clo* mutant. The severity of the interrenal fusion phenotype seemed to be correlated with that of the vascular disruption. While about 97% of uninjected control embryos displayed normal interrenal laterality (n = 116), 89% of *ets1b* morphants lost interrenal laterality (n = 106), ranging from defective relocalization after the convergence to unsuccessful medial migration (Table 1). The aberrant interrenal morphology in the vasculature-deficient embryo was not similar to the interrenal phenotype in the *tnnt2* morphant (a representative sample shown in Fig. 2E–E″,F). It is to be noted that in the absence of blood flow, the interrenal tissue remained juxtaposed between the DA and the PCV. Hence, we conclude that the formation of trunk vasculature near the interrenal region, but not vascular flow, might play a role in the laterality, or right-sidedness, of the fused interrenal tissue. Furthermore, phenotypic differences among the *clo* mutant, the *ets1b* morphant, and their wild type controls implied that the interrenal fusion at the midline and the later interrenal relocalization might occur as two distinct yet consecutive phases, differentially regulated by pre-vascular angioblasts and vascular ECs, respectively. To further examine whether arterial or venous vasculature plays a specific role in relocalization and laterality of the interrenal tissue, in the following experiments we checked the interrenal morphology in embryos deficient in either arterial or venous cells.

Inhibition of Artery Formation Led to Defective Relocalization and Laterality of the Interrenal Tissue

To manipulate arterial- versus venous-differentiation, the expression of *grl*/*hey2* was altered following what was reported by Zhong at al. (2001). Our earlier study showed that in *fli1* promoter-driven fluorescent embryos injected with the antisense morpholino oligo against *hey2*, medial migration and midline fusion of bilateral interrenal primordia were not affected, arguing against a specific role for arterial ECs to regulate the early interrenal convergence. It, however, remains unclear whether artery would pattern developmental relocalization and right-sided laterality of the interrenal tissue. To examine how the peri-interrenal vasculature reacts to the inhibition of *hey2* expression, we injected *hey2* morpholino at the dosage of about 1.2 pmol per embryo into wild type embryos, and the morphants manifesting notable vascular defects by a complete loss of circulation (53.1%; n = 143) were selected for the subsequent examination of either arterial- or venous-specific markers by ISH. Ventral flat-mount views showed that while the arterial-specific gene *eph-B2a* was abundantly expressed at the glomeruous and the DA in the control embryo at 35 hpf (Fig. 3Aa), it was absent at the DA and poorly expressed in the glomerular region of all the *hey2* morphants checked (n = 45; Fig. 3Ab). Conversely, the venous-specific gene *flt4* was excessively expressed at the PCV and its two bilateral branches in the *hey2* morphant, thus showing a malformed venous structure at the midtrunk (n = 31; Fig. 3Ad). The effects of *hey2* morpholino on the artery and vein were consistent with the data reported by Zhong et al. (2001). It is shown in Figure 3Aa that the laterally-positioned interrenal tissue was intimately associated with the arterial ECs that constitute the pronephric glomerulous and the DA. It is interesting to note that, albeit evident in its laterality, the *ff1b*-expressing interrenal tissue was in contact with both right and left branches of the PCV, implying a possible asymmetry of PCV structure at the midtrunk area. The *ff1b*-expressing interrenal tissue in 95% of the *hey2* morphants, which showed absence of circulation, was shown as a single cluster lying across the midline, with the centrally-positioned interrenal tissue juxtaposed between two branches of PCV (Fig. 3Ab,d). The intensity of *ff1b* expression did not appear to be reduced upon the disruption of its adjacent arterial vasculature. Our

Fig. 2. Effects of the *ets1b* antisense morpholino injection on the interrenal tissue and its neighboring vasculature. Confocal sections showing the interrenal tissue as detected by 3 β-Hsd activity staining (**A–E**), and the neighboring endothelium as labeled by green fluorescence (**A′–E′**), of 2-dpf *Tg(fli1:EGFP)*^{Y1} embryos uninjected (A), injected with *ets1b*MO (B–D), or with *tnnt2*MO (E), respectively. **A″–E″**: The merged images of 3 β-Hsd activity staining and GFP. A–E are dorsal views with anterior oriented to the top. **F**: The merged image of 3 β-Hsd staining and GFP of the same embryo as in E–E″, a lateral view with anterior to the left. B–B″, C–C″, D–D″: Classes I to III of interrenal phenotypes in the *ets1b* morphant, where the trunk endothelium was reduced and the axial vascular formation inhibited. Vascular ECs, but not the blood flow, are required for the convergence and laterality of the interrenal tissue. Yellow dotted lines indicate the position of the midline. Orange arrows, interrenal tissues; yellow arrowheads, angiogenic glomerulus; DA, dorsal aorta; PCV, posterior cardinal vein; ISV, intersegmental vessel. Scale bar = 50 μM.

Fig. 3. Effects of the *hey2* antisense morpholino injection on the interrenal tissue and its neighboring vasculature. **A**: Ventral flat-mount views showing the effects of *hey2*MO on the expressions of *eph-B2a* and *flt4* in the peri-interrenal region. Uninjected control (**a,c**) and injected embryos (**b,d**) were fixed at 35 hpf, and two-color ISH were carried out to detect the expression of *ff1b* together with either *eph-B2a* (a,b) or *flt4* (c,d). a–d: Oriented with anterior to the top. **B**: Confocal images display the interrenal tissue as detected by 3 β-Hsd activity staining (left panels, **a–f**), and the neighboring endothelium as labeled by green fluorescence (middle panels, **a′–f′**), of 34-hpf (a,b) and 54-hpf (c–f) *Tg(kdrl:EGFP)*^{s843} embryos uninjected (a–d) or injected with *hey2* antisense morpholino (e,f). The merged images of 3 β-Hsd activity staining and GFP are shown in the right panels (**a″–f″**). Each fluorescent image depicting the vascular morphology represents a projection of a consecutive z-stack encompassing the depth of the interrenal tissue. a–a″, c–c″, e–e″ are dorsal views with anterior oriented to the top, while b–b″, d–d″, f–f″ are dorsolateral views with anterior to the right. Relocalization and right-sided laterality of the interrenal tissue is perturbed upon the disruption of axial artery in the *hey2* morphant. Black and orange arrows indicate the *ff1b*-expressing and steroidogenic interrenal tissues, respectively. Red and blue arrowheads denote the arterial and venous vasculature, respectively. Yellow and blue dotted lines, boundaries of arterial and venous structures, respectively; white dotted lines, position of the midline; DA, dorsal aorta; ISV, intersegmental vessel; PCV, posterior cardinal vein; DC, duct of Cuvier; G, glomerulus; IR, interrenal tissue. Scale bar = 50 μM.

TABLE 2. Phenotypic Statistics of 34-hpf *Tg(kdrl:EGFP)*^{s843} Embryos Injected by Either *hey2* Antisense Morpholino Oligonucleotide or *hey2* mRNA

	Control		*hey2*MO		*hey2* mRNA	
Phenotype	No.	(%)	No.	(%)	No.	(%)
Bilateral clusters widely across the midline	0		0		76	(30.2)
Bilateral clusters immediately across the midline	2	(1.4)	2	(3.2)	45	(17.9)
Single cluster at the central midline	0		60	(95.2)	74	(29.4)
Single cluster to the left of the midline	7	(5.0)	0		38	(15.1)
Single cluster to the right of the midline	131	(93.6)	1	(1.6)	19	(7.5)
Total	140		63		252	

ISH results thus revealed that while the artery formation was inhibited in the *hey2* morphant, lateral relocalization of the *ff1b*-expressing interrenal cells was perturbed, culminating in a single interrenal tissue positioned at the central midline.

To examine how the inhibition of arterial fate decision would affect morphology of the functionally-differentiated steroidogenic interrenal tissue, as well as the three-dimensional vascular pattern in the peri-interrenal area, *hey2* morpholino was injected into *Tg(kdrl:EGFP)*^{s843} where the EGFP fluorescence is driven by the zebrafish *kinase insert domain receptor like* (*kdrl*) promoter (Jin et al., 2005). In the control embryo at 34 hr post-fertilization (hpf), part of the fused and lateralized interrenal tissue lies immediately ventral to the DA and caudal to the pronephric glomerulus (Fig. 3Ba–a″, b–b″). At 54 hpf, the entire interrenal tissue relocated slightly rightwards as viewed dorsally, and was positioned immediately lateral to the DA and tightly associated with the right branch of the PCV (Fig. 3Bc–c″, d–d″). In the dorsolateral view of wild-type embryos at 34 and 54 hpf, the interrenal tissue was situated ventral to the DA and dorsal to the PCV (Fig. 3Bb″,d″). Consistent with the ISH results in Figure 3A, assembly of the DA was disrupted in the *hey2* morphant, which lacks circulation, and the ISV was absent (Fig. 3Be′,f′). As compared with the control embryo, the DA structure dorsal to the interrenal tissue was severely disrupted (Fig. 3Bf″). In contrast with the severe disruption of the DA, the presence of the PCV and the duct of Cuvier was still evident in the *hey2* morphant (Fig. 3Be″). The interrenal tissue in the *hey2* morphant remained tightly associated with the PCV (Fig. 3Be″,f″), and was shown as a single cluster lying at the central midline (Fig. 3Be″) in more than 95% of the *hey2* morphants which displayed disrupted vasculature and loss of blood flow (n = 63; Table 2). The interrenal morphology of the *hey2* morphant suggested that formation of the DA might be essential for lateral relocalization of the interrenal tissue after the medial fusion.

Inhibition of Vein Formation Led to Defective Interrenal Morphogenetic Movements With a Range of Expressivities

In order to examine the role of venous vessels for morphogenetic movements of the interrenal tissue, the overexpression of *hey2* mRNA was utilized to inhibit venous vessel formation (Zhong et al., 2001). At the dosage of approximately 200 pg per embryo, the injection of *hey2*-capped mRNA into the wild type embryo led to a complete absence of blood circulation (43.3%, n = 157). To assess whether the *hey2* mRNA injection could efficiently and specifically inhibit the formation of venous vasculature in the peri-interrenal region, we examined the expression pattern of *eph-B2a* (Fig. 4Aa–f) and *flt4* (Fig. 4Ag–l) genes, respectively, with ISH. Each was assayed simultaneously with that of *ff1b* to mark the location of interrenal cells. Ventral flat-mount views showed that while the *flt4* expression was absent in the *hey2*-injected embryo at 35 hpf (n = 29; phenotypic classes shown in Fig. 4Ab–f), the *eph-B2a* expression could be clearly detected in the peri-interrenal region (n = 39; phenotypic classes shown in Fig. 4Ah–l). The *eph-B2a* expression in the *hey2*-injected embryo suggested a malformed arterial structure with variable expressivities, which, however, remained tightly associated with the *ff1b*-expressing interrenal cells (Fig. 4Ah–l). We classified *hey2* dominant-positive phenotypes into classes I to V, based on different locations of the interrenal tissue with respect to the midline. In classes I and II of the injected embryos, various degrees of interrenal migration defects were shown (Fig. 4Ab,c,h,i), while interrenal phenotypes in classes III and IV might have resulted from a disrupted laterality (Fig. 4Ad,e,j,k). Although the interrenal tissue in class-V embryos displayed normal laterality, its adjacent arterial vasculature was malformed (Fig. 4Al).

To evaluate the penetrance and expressivity of the interrenal phenotype upon the inhibition of venous formation, in the context of three-dimensional vascular architecture surrounding the interrenal tissue, the *hey2* mRNA was injected into *Tg(kdrl:EGFP)*^{s843} embryos for the subsequent 3βHsd activity staining. Consistent with the ISH results in Figure 4A, specific inhibition of venous formation was observed in all the injected embryos where the blood flow was absent (Fig. 4Bc′–l′). Concomitant with a severe disruption of the PCV structure at the peri-interrenal area, unsuccessful central assembly of the DA structure was detected in classes I, II, IV, and V (Fig. 4Bc′–f′,i′–l′). It was speculated that assembly defects of the DA in

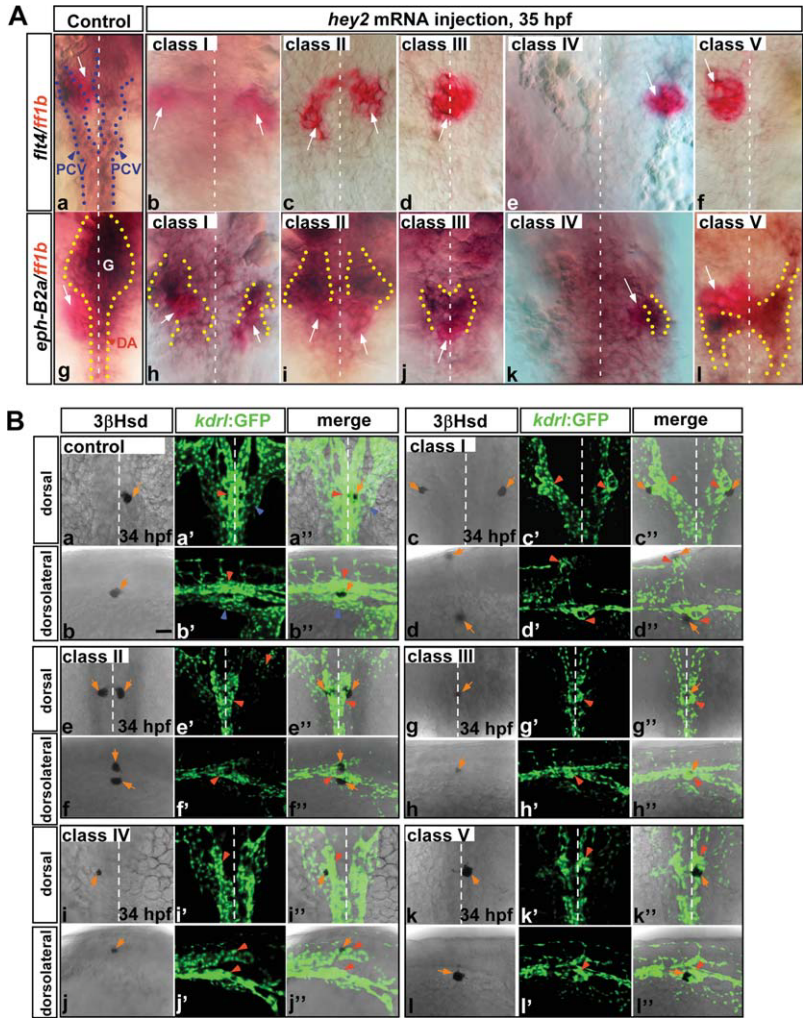

Fig. 4. Effects of *hey2* mRNA injections on the interrenal tissue and its neighboring artery and vein. **A**: Effects of *hey2* mRNA on the expressions of *flt4* and *eph-B2a* in the peri-interrenal region. Uninjected control (a, g) and injected embryos (b–f, h–l) were fixed at 35 hpf and subject to two-color ISH for detecting the expression of *ff1b* together with that of either *flt4* (**a–f**) or *eph-B2a* (**g–l**). All panels in A are ventral views with anterior oriented to the top. The *flt4* expression at the peri-interrenal area is absent in all phenotypic classes of injected embryos (classes I–V). **B**: Sets of confocal images display the interrenal tissues as detected by 3 β-Hsd activity staining (left panels of each set, a–l), and the neighboring endothelium as labeled by green fluorescence (middle panels of each set, **a′–l′**), of 34-hpf *Tg(kdrl:EGFP)*^{s843} embryos uninjected (a, b) or injected with *hey2* mRNA (c–l, classes I–V). The merged images of 3 β-Hsd activity staining and GFP are shown in the right panels of each set (**a″–l″**). Each fluorescent image depicting the vascular morphology represents a projection of a consecutive z-stack encompassing the depth of the interrenal tissue. a, c, e, g, i, k are dorsal views with anterior oriented to the top, while b, d, f, h, j, l are dorsolateral views with anterior to the right. The venous endothelium at the peri-interrenal area is severely reduced in all classes of *hey2* mRNA-injected embryos, which is accompanied by various expressivities of the interrenal morphogenetic defect. White and orange arrows, *ff1b*-expressing and steroidogenic interrenal tissues; red and blue arrowheads, artery and vein, respectively; blue and yellow dotted lines, boundaries of venous and arterial structures, respectively; white dotted lines, position of the midline; DA, dorsal aorta; PCV, posterior cardinal vein; G, glomerulus. Scale bar = 50 μM.

classes I, II, IV, and V could be due to an ectopic early effect of the *hey2* mRNA overexpression on the general convergence movement, which did not affect functional differentiation of the steroidogenic interrenal cells. Although assembly of the DA appeared to be normal in the class-III embryo (Fig. 4Bg′,h′), the amount of the arterial endothelium seemed to be less than that in the control embryo (Fig. 4Ba′,b′). In classes I and II, the severity of the DA assembly defect was correlated with that of the interrenal medial migration (Fig. 4Bc″,e″). In classes IV and V, a single interrenal tissue was associated with either the left (class IV) or the right (class V) of bilateral DA structures that failed to assemble centrally (Fig. 4Bi″,j″,k″,l″). It remains unclear whether the left-sided interrenal laterality in class IV was due to a defective fusion position of bilateral interrenal primordia, or to a randomized relocalization after midline fusion, or to a defective differentiation of the right interrenal cluster that did not migrate centrally. In class III, assembly of the DA as well as midline fusion of bilateral interrenal tissues were both successful, while lateral relocalization of the converged interrenal tissue was defective, culminating in a single interrenal tissue embedded within the DA at a level slightly posterior to the bifurcation point (Fig. 4Bg–g″,h–h″). The statistics for class I to V interrenal phenotypes in the experiment described above is summarized in Table 2. Our results thus suggest that the simultaneous presence of the DA and PCV branches is essential for developmental relocalization and laterality of the interrenal tissue.

Examination of the interrenal morphology, in a scenario where arterial versus venous formation was manipulated, led us to conclude that the existence of both the DA and the PCV was required for defining laterality of the interrenal tissue after the initial interrenal convergence and fusion. While the interrenal tissue in the artery-deficient embryo failed to relocate laterally, that in the vein-deficient embryo demonstrated a wide range of expressivities in terms of morphogenetic movements. It is interesting to note that the location of the interrenal tissue relative to the midline appeared to be correlated with the severity of arterial assembly defects, in all phenotypic classes of vein-deficient embryos (Fig. 4B). Phenotypic differences of the interrenal phenotype between artery-deficient and vein-deficient embryos might be in part explained by the fact that although the axial venous vasculature in the *hey2* morphant was hypomorphic, central assembly of the PCV was less perturbed (Fig. 3Ad, Be′,f′). As interrenal cells demonstrated affinities for both

arterial and venous ECs, in wild-type as well as manipulated embryos, it remains unclear whether relocalization and laterality of the interrenal tissue requires a simultaneous close association with both arterial and venous ECs. It is tempting to speculate that the presence of the DA and the PCV near the interrenal tissue might serve as vessel coordinates to define interrenal laterality. In this regard, the arterial versus venous fate specification might not be essential for guiding the interrenal morhogenetic movement. However, the results of our study could not explicitly address this question, as manipulation of the arterial versus venous fate by altering expression levels of *hey2* also led to a disruption of the vascular architecture at the midtrunk. Specifically for the midtrunk area, it remains to be explored whether and how the arterial versus venous fate decision could be manipulated without altering the vascular architecture.

In summary, we dissected in this study early morphogenetic steps of the interrenal primordial cells. Histological analysis upon various fashions of vascular disruption revealed an intimate interaction between interrenal cells and its adjacent endothelium, at each step of the interrenal morphogenetic movements. Furthermore, shaping of the embryonic interrenal morphology was secondary to and directed by ECs during the process of vascular assembly, while the architecture of both arterial and venous vessels at the midtrunk was essential for defining laterality of the interrenal tissue.

The Relationship Between Blood Vessels and a General Asymmetry Program in Patterning Laterality of the Interrenal Tissue

While our results indicate the importance of vascular topology at the midtrunk to pattern the interrenal laterality, our experiments did not answer the question of why the interrenal tissue was relocalized toward the right, rather than the left, of the midline. It remains to be explored whether the intimate interaction between the interrenal tissue and its adjacent artery and vein has to function, in conjunction with a general asymmetry molecular program, to determine the interrenal laterality. In our previous studies, it was found that central migration of bilateral interrenal tissues was defective in Nodal mutants *one-eyed pinhead* (*oep*) and *squint* (*sqt*) (Chai et al., 2003; Liu et al., 2003). However, multiple levels of developmental defects other than a loss of asymmetry are caused by the mutation of either *oep* or *sqt*, which include disruption of the endoderm and the axial vasculature (Alexander and Stainier, 1999; Brown et al., 2000). Therefore, a more comprehensive study of those gene that govern the general asymmetry program should be performed, in order to understand the specific influence of left-right axis formation on the interrenal tissue and its nascent vasculature. Our preliminary results showed that a randomization of interrenal laterality was observed in *polycystin-2* (*pkd2*) morphants, where the specification of left-right asymmetry was perturbed without obviously disrupting the midtrunk vasculature (data not shown). *pkd2* is expressed at the zebrafish brain, pronephros, and Kupffer's vesicle to regulate cilia-driven fluid flow, and whose function in the Kupffer's vesicle is required for establishing the organ situs (Kramer-Zucker et al., 2005). While *pkd2* is also important for the pronephric fluid flow, it awaits further clarification as to whether its specific function at Kupffer's vesicle regulates the interrenal laterality. Furthermore, it is to be examined how other members of the asymmetry program, such as *nodal*-related gene *southpaw* (Long et al., 2003), *lefty*-related genes *lefty1* and *lefty2* (Bisgrove et al., 1999; Wang and Yost, 2008), would function in patterning laterality of the interrenal tissue, and whether the interrenal laterality could be due to a possible asymmetry of the midtrunk vasculature.

As our results indicate that embryonic vessels might be involved in patterning interrenal laterality, it would be interesting to explore whether the same mechanism might participate in other aspects of organogenesis. While the budding of embryonic liver and pancreas from the developing gut occurs at the level posterior to the interrenal tissue at the midtrunk, the direction of outgrowth as well as laterality for these two digestive organs are unaffected in the endothelium-free *clo* mutant (Field et al., 2003a,b). The initial medial movement of cardiomyocytes was not affected in *clo*, yet the absence of endocardium leads to a later defect in the assembly and elongation of the heart tube (Holtzman et al., 2007). Nevertheless, laterality of the heart tube during its assembly is not aberrant in *clo*. Therefore, it remains unclear why laterality of the interrenal tissue, among other organs, could be particularly influenced by the vascular morphology. Unlike its mammalian counterpart, the interrenal tissue is formed not as a discrete organ in teleosts, with no formation of distinct steroidogenic zones during its development (Grassi Milano et al., 1997). While the outer cortex and inner medulla of the mammalian adrenal gland are well separated with clear boundaries formed in between, interrenal and chromaffin cells integrate to form the interrenal organ through intermingling of two cell populations (Grassi Milano et al., 1997; Chai et al., 2003; To et al., 2006). Extracellular matrix proteins Laminin, Collagen IV, and Fibronectin, as well as their Integrin receptors, are differentially expressed in various domains within the human fetal adrenal gland to coordinate specific steroidogenic pathways and cell turnover during development (Chamoux et al., 2001, 2002). The formation of basement membrane is evident, along with the distribution of laminin isoforms, in the fetal as well as the adult human adrenal gland (Virtanen et al., 2003). In contrast, the interrenal tissue in teleosts demonstrated high morphological plasticity during development, which might be correlated with a lack of stabilized basement membrane on its own. Hypothetically, peri-interrenal vessels might modulate the interrenal morphology through providing the basement membrane. Therefore, it remains to be investigated whether the basement membrane with its extracellular matrix (ECM) components is formed within the interrenal organ, or at the junction between the interrenal cell and its adjacent endothelium. Prospectively, elucidation of the pattern of ECM deposition at the interrenal and peri-interrenal

regions might shed some light on how vessels shape the interrenal tissue in the early zebrafish embryo.

EXPERIMENTAL PROCEDURES

Zebrafish Strains and Growth Conditions

Zebrafish (*Danio rerio*) were raised according to standard protocols (Westerfield, 2000). Embryos were obtained by natural spawning and cultured in embryo medium at 28.5°C. Staging of the embryos was carried out as previously described (Kimmel et al., 1995). Embryos to be subject to histological analysis were treated with 0.03% phenylthiourea (Sigma, St. Louis, MO) from 12 hpf onwards to inhibit pigment formation. *Tg(ff1bEx2:GFP)*, where a GFP cassette was inserted into exon2 of the *ff1b* locus, was developed through a BAC transgenesis strategy (Quek, 2009). A study describing the technical details and characterization of this line is currently underway. The *Tg(fli1:EGFP)*^{Y1} line was from the Zebrafish International Resource Center (Eugene, OR). The *Tg(kdrl:EGFP)*^{s843} line was a kind gift from Didier Stainier (San Francisco, CA).

Whole-Mount In-Situ Hybridization

Whole-mount in situ hybridization (ISH) was performed as described with minor modifications (Liu et al., 2003). Digoxigenin-labeled riboprobes were synthesized from plasmids containing cDNAs for *eph-B2a* and *flt4*. *eph-B2a* plasmid was linearized with *Sal*I and transcribed with *SP6* RNA polymerase. *flt4* plasmid was linearized with *Eco*RI and transcribed with *T7* RNA polymerase. Fluorescein-labeled riboprobes were synthesized from *Sal*I linearized *ff1b* plasmids and transcribed with *T7* RNA polymerase. DIG-labeled riboprobes were detected with alkaline phosphatase conjugated anti-DIG antibody (Roche, Nutley, NJ) while Fluorescein-labeled probes were detected by alkaline phosphatase conjugated anti-Fluorescein antibody (Roche). For one-color ISH, visualization of *ff1b* expression was performed with BCIP/TNBT (Chemicon, Temecula, CA). For two-color ISH, visualization of either *eph-B2a* or *flt4* expression was performed with BCIP/TNBT (Chemicon), and *ff1b* expression was stained with Fast Red (Roche) subsequently. The inactivation of the first antibody in two-color ISH was performed by heating the stained embryos at 65°C for 30 min. Stained embryos were post-fixed in 4% paraformaldehyde (PFA) in PBS and washed in PBS supplemented with 1% of Tween20 (PBST). This was followed by tissue clarification in 50% glycerol in PBS. Specimens were mounted on glass slides and photographed under Nomaski optics on an Olympus BX51 microscope system.

Microinjection of Morpholino Oligonucleotide and mRNA

To analyze how various types of endothelial defects affect the interrenal morphology, morpholino oligonucleotides (MO) were synthesized at Genetools LLC and diluted in 1 × Danieau solution before microinjections. The nucleotide sequences of the *ets1b*MO1, *ets1b*MO2, *tnnt2*MO, and *hey2*MO are 5′ – TTG GTA CAT TTC CAT ATC TTA AAG T - 3′ (Sumanas and Lin, 2006), 5′ – CAC TGA GTC CTT ATT TCA CTA TAT C - 3′ (Sumanas and Lin, 2006), 5′-CAT GTT TGC TCT GAT CTG ACA CGC A-3′ (Sehnert et al., 2002), and 5′-CGC GCA GGT ACA GAC ACC AAA AAC T-3′ (Zhong et al., 2001), respectively. Zebrafish *hey2* full-length cDNA clone (MGC:136746) was obtained from Open Biosystems and the ORF was subcloned into pCS2+. Capped mRNA of *hey2* was in vitro transcribed from the linearized plasmid by using Message Machine (Ambion, Austin, TX). MO- or mRNA-containing solutions (~2.3 nL) were injected into one- to two-cell-stage embryos by using a Nanoject (Drummond, Broomall, PA).

Histology and Microscopy

For monitoring dynamic morphogenetic movements of the interrenal tissue in the live embryo, time-lapse confocal imaging was performed to collect fluorescent images from *Tg(ff1bEx2:GFP)* embryos anesthetized by tricane, using a Zeiss Axioplan II microscope equipped with LSM 510 META and an objective lens (×10 N.A. 0.3) (Carl Zeiss Inc., Thornwood, NY). Images were acquired as a z stack (8-μM slices) and assembled as a 3D projection. To delineate the morphology of the steroidogenic interrenal tissue, histochemical staining for 3β-Hydroxysteroid dehydrogenase/Δ5-Δ4-isomerase (3β-Hsd) was performed on whole embryos as previously described (Grassi Milano et al., 1997). For simultaneous analysis of interrenal steroidogenic activity and endothelial GFP fluorescence, 3β-Hsd staining signals were captured using transmitted light, while the fluorescent signals were captured with an Argon 488-nm laser connected to the confocal microscope. Image processing and analysis were performed using the LSM 510 version 3.5 software.

ACKNOWLEDGMENTS

We thank Prof. Didier Stainier for the kind gift of *Tg(kdrl:EGFP)*^{s843} strain; Dr. Sheng-Ping Huang, Dr. Cheng-Chen Huang, Dr. Yung-Jen Chuang, Ms Lisa Chen, Dr. Maysu You, Dr. Yun-Jin Jiang, and Prof. Bon-chu Chung for generous support in aquaculture; Dr. Seng-Sheen Fan and his team for expert assistance on confocal microscopy. Sue-Ing Quek was supported by a NUS Postgraduate Research Scholarship.

REFERENCES

Alexander J, Stainier DY. 1999. A molecular pathway leading to endoderm formation in zebrafish. Curr Biol 9:1147–1157.

Alt B, Elsalini OA, Schrumpf P, Haufs N, Lawson ND, Schwabe GC, Mundlos S, Grüters A, Krude H, Rohr KB. 2006. Arteries define the position of the thyroid gland during its developmental relocalisation. Development 133:3797–3804.

Bisgrove BW, Essner JJ, Yost HJ. 1999. Regulation of midline development by antagonism of lefty and nodal signaling. Development 126:3253–3262.

Brown LA, Rodaway AR, Schilling TF, Jowett T, Ingham PW, Patient RK, Sharrocks AD. 2000. Insights into early vasculogenesis revealed by expression of the ETS-domain transcription factor Fli-1 in wild-type and mutant zebrafish embryos. Mech Dev 90:237–252.

Chai C, Liu YW, Chan WK. 2003. ff1b is required for the development of steroidogenic component of the zebrafish interrenal organ. Dev Biol 260:226–244.

Chamoux E, Bolduc L, Lehoux JG, Gallo-Payet N. 2001. Identification of extracellular matrix components and their integrin receptors in the human fetal adrenal gland. J Clin Endocrinol Metab 86:2090–2098.

Chamoux E, Narcy A, Lehoux JG, Gallo-Payet N. 2002. Fibronectin, laminin, and collagen IV as modulators of cell behavior during adrenal gland development in the human fetus. J Clin Endocrinol Metab 87:1819–1828.

Cleaver O, Melton DA. 2003. Endothelial signaling during development. Nat Med 9:661–668.

Field HA, Dong PD, Beis D, Stainier DY. 2003a. Formation of the digestive system in zebrafish. II. Pancreas morphogenesis. Dev Biol 261:197–208.

Field HA, Ober EA, Roeser T, Stainier DY. 2003b. Formation of the digestive system in zebrafish. I. Liver morphogenesis. Dev Biol 253:279–290.

Grassi Milano E, Basari F, Chimenti C. 1997. Adrenocortical and adrenomedullary homologs in eight Species of adult and developing teleosts: morphology, histology, and immunohistochemistry. Gen Com Endocrinol 108: 483–496.

Holtzman NG, Schoenebeck JJ, Tsai HJ, Yelon D. 2007. Endocardium is necessary for cardiomyocyte movement during heart tube assembly. Development 134:2379–2386.

Hsu HJ, Lin G, Chung BC. 2003. Parallel early development of zebrafish interrenal glands and pronephros: differential control by wt1 and ff1b. Development 130:2107–2116.

Jin SW, Beis D, Mitchell T, Chen JN, Stainier DY. 2005. Cellular and molecular analyses of vascular tube and lumen formation in zebrafish. Development 132:5199–5209.

Kimmel CB, Ballard WW, Kimmer SR, Ullmann B, Schilling TF. 1995. Stages of embryonic development of the zebrafish. Dev Dyn 203:253–310.

Kramer-Zucker AG, Olale F, Haycraft CJ, Yoder BK, Schier AF, Drummond IA. 2005. Cilia-driven fluid flow in the zebrafish pronephros, brain and Kupffer's vesicle is required for normal organogenesis. Development 132:1907–1921.

Lawson ND, Weinstein BM. 2002. In vivo imaging of embryonic vascular development using transgenic zebrafish. Dev Biol 248:307–318.

Liu YW. 2007. Interrenal organogenesis in the zebrafish model. Organogenesis. 3:44–48.

Liu YW, Guo L. 2006. Endothelium is required for the promotion of interrenal morphogenetic movement during early zebrafish development. Dev Biol 297: 44–58.

Liu YW, Gao W, The HL, Tan JH, Chan WK. 2003. Prox1 is a novel coregulator of Ff1b and is involved in the embryonic development of the zebra fish interrenal primordium. Mol Cell Biol 23:7243–7255.

Long S, Ahmad N, Rebagliati M. 2003. The zebrafish nodal-related gene southpaw is required for visceral and diencephalic left-right asymmetry. Development 130:2303–2316.

Nikolova G, Strilic B, Lammert E. 2007. The vascular niche and its basement membrane. Trends Cell Biol 17: 19–25.

Quek SI. 2009. Molecular characterization of the zebrafish *ff1b* gene. Ph.D. thesis. National University of Singapore.

Red-Horse K, Crawford Y, Shojaei F, Ferrara N. 2007. Endothelium-microenvironment Interactions in the developing embryo and in the adult. Dev Cell 12:181–194.

Sakaguchi TF, Sadler KC, Crosnier C, Stainier DY. 2008. Endothelial signals modulate hepatocyte apicobasal polarization in zebrafish. Curr Biol 18:1565–1571.

Sehnert AJ, Huq A, Weinstein BM, Walker C, Fishman M, Stainier DY. 2002. Cardiac troponin T is essential in sarcomere assembly and cardiac contractility. Nat Genet 31:106–110.

Serluca FC, Drummond IA, Fishman MC. 2002. Endothelial signaling in kidney morphogenesis: a role for hemodynamic forces. Curr Biol 12:492–497.

Sumanas S, Lin S. 2006. Ets1-related protein is a key regulator of vasculogenesis in zebrafish. PLoS Biol 4:e10.

To TT, Hahner S, Nica G, Rohr KB, Hammerschmidt M, Winkler C, Allolio B. 2007. Pituitary-interrenal interaction in zebrafish interrenal organ development. Mol Endocrinol 21:472–485.

Virtanen I, Korhonen M, Petäjäniemi N, Karhunen T, Thornell LE, Sorokin LM, Konttinen YT. 2003. Laminin isoforms in fetal and adult human adrenal cortex. J Clin Endocrinol Metab 88: 4960–4966.

Wang X, Yost HJ. 2008. Initiation and propagation of posterior to anterior (PA) waves in zebrafish left-right development. Dev Dyn 237:3640–3647.

Westerfield M. 2000. The zebrafish book: guide for the laboratory use of zebrafish (*Danio rerio*), 4th ed. Eugene, OR: University of Oregon Press.

Zhong TP, Childs S, Leu JP, Fishman MC. 2001. Gridlock signalling pathway fashions the first embryonic artery. Nature 414:216–220.